

# ADVANCED MAGNETIC FIELD DESCRIPTION AND MEASUREMENTS ON CURVED ACCELERATOR MAGNETS

P. Schnizer, E. Fischer, A. Mierau, GSI, Darmstadt, Germany  
B. Schnizer, Technische Universität Graz, Graz, Austria  
P. Akishin, JINR, Dubna, Moscow Region, Russia

## Abstract

The SIS100 accelerator will be built within the first realisation phase of the FAIR project. The series production of its superconducting bending magnets was started without any test model in 2013. This time saving strategy requires a careful investigation of the magnetic field quality for the first manufactured dipole. The consequences of the curved magnet design was analysed developing advanced multipoles for elliptical and toroidal magnet geometries. We present the theoretical results together with measured data obtained for the first of series dipole. A description of the rotating coil probe based measurement method will be given together with the achieved field quality as well as an estimation of the limits of the chosen field representation and its beam dynamics interpretation.

## INTRODUCTION

The beam pipe aperture of the SIS100 dipole is to a large extent covered by the ion particle beam. Given that the magnet is of small size a proper understanding of the harmonics content is required to forecast the machine performance. The standard method, the search coil probes, used for qualifying conventional magnets, which measure the field on the mid plane, will not allow calculating harmonics reliably. Further the SIS100 magnets are superconducting and thus sliding a coil probe on an air cushion system is not applicable.

These demands were tackled extending the rotating coil probe measurement method to elliptical apertures [1] and curved magnets [2].

## THEORY

### Cylindric Elliptic Multipoles

In a magnet with a rectangular gap an ellipse as reference curve covers a larger area than a circle [1, 3]. So it is advantageous to use elliptic coordinates  $x = e \cosh \eta \cos \psi$  and  $y = e \sinh \eta \sin \psi$ , with  $a, b$  and  $e = \sqrt{a^2 - b^2}$  the major, minor semi-axes and the eccentricity of the reference ellipse, which is expressed in the above coordinates by  $\eta_0 = \tanh^{-1}(b/a)$ . The Cartesian and the elliptic coordinates are connected by a conformal map:

$$\mathbf{z} = x + iy = e \cosh(\eta + i\psi) = e \cosh \mathbf{w}. \quad (1)$$

Solving the potential equation by separation leads to hyperbolic functions in  $\eta$  and trigonometric functions in  $\psi$ . The

complex field expansion is  $\mathbf{B}(\mathbf{w}) = B_y(\eta, \psi) + iB_x(\eta, \psi)$ :

$$\mathbf{B}(\mathbf{w}) = B_0 \left( \frac{\mathbf{E}_0}{2} + \sum_{n=1}^M \mathbf{E}_n \frac{\cosh[n(\eta + i\psi)]}{\cosh(n\eta_0)} \right).$$

In view of the transformation (1) expansions for the same field are related. In fact:

$$\begin{aligned} \cosh[n(\eta + i\psi)] &= \cosh(n\eta) \cos(n\psi) + i \sinh(n\eta) \sin(n\psi) \\ &= \sum_{m=0}^n [\operatorname{Re}(t_{m,n} z^m) + i \operatorname{Im}(t_{m,n} z^m)] \end{aligned} \quad (2)$$

with the residue

$$t_{mn} = \operatorname{Res} \left( \sinh \mathbf{w} \cosh(n\mathbf{w}) / \cosh^{m+1} \mathbf{w}, \mathbf{w} = i\pi/2 \right). \quad (3)$$

Also from the values for the  $\mathbf{E}_n$  values for the  $\mathbf{C}_m$  may be found.

### Toroidal Circular Multipoles

Rotating coil probes integrate the field along their axis. To judge if these can be used for measuring a curved magnets, a field description following the curvature but invariant to this coordinate is required. Local Toroidal coordinates [2] are obtained by rotating off-centre dimensionless polar coordinates  $\rho, \vartheta$  by an angle  $\varphi$ :

$$\begin{aligned} X + iY &= R_C h e^{i\varphi}, & Z &= R_{Ref} \sin \vartheta, \\ h &= 1 + \epsilon \rho \cos \vartheta & \epsilon &= R_{Ref}/R_C \end{aligned}$$

$R_C$  = major radius = radius of curvature;  $R_{Ref}$  = minor radius = reference radius;  $\epsilon$  the inverse aspect ratio. The Cartesian coordinates  $X, Y, Z$  are centred in the torus centre;  $Z$  is normal to the equatorial plane.

The approximate solutions of the potential equation obtained by the approximate R-separation are:  $\Phi_m = h^{-1/2} \rho^m e^{im\vartheta}$ ,  $m = 0, 1, 2, \dots$ . Introducing Cartesian coordinates  $x', y'$  in the plane  $\varphi = \text{const}$ :

$$\mathbf{z}' = x' + iy' = R_{Ref} \rho e^{i\vartheta} \quad (4)$$

we get the approximate circular toroidal multipoles:

$$\Phi_m(x', y') = \left( \frac{\mathbf{z}'}{R_{Ref}} \right)^m - \frac{\epsilon}{4} \left[ \left( \frac{\mathbf{z}'}{R_{Ref}} \right)^{m+1} + \left( \frac{\mathbf{z}'}{R_{Ref}} \right)^{m-1} \frac{|\mathbf{z}'|^2}{R_{Ref}^2} \right]. \quad (5)$$

Corresponding (normal and skew) vector fields are ( $m = 1, 2, \dots$ ):

$$\begin{aligned} \vec{T}_m(x', y') &= -\frac{R_{Ref}}{m} \nabla' \Phi_m(x', y'), \\ \vec{T}_m^{(n)}(x', y') &= \operatorname{Re}(\vec{T}_m(x', y')), \quad \vec{T}_m^{(s)}(x', y') = \operatorname{Im}(\vec{T}_m(x', y')). \end{aligned}$$

The basis vectors can be given in full form as

$$\begin{pmatrix} \vec{\mathbf{T}}_m^{(n)} \\ \vec{\mathbf{T}}_m^{(s)} \\ \vec{\mathbf{T}}_m \end{pmatrix} = \left( \frac{|z'|}{R_{Ref}} \right)^2 \frac{(m-1)}{m} \left( \frac{z'}{R_{Ref}} \right)^{m-2} \quad (6)$$

$$+ \frac{2\vec{z}'}{mR_{Ref}} \begin{pmatrix} i \operatorname{Im} \left( (z'/R_{Ref})^{m-1} \right) \\ \operatorname{Re} \left( (z'/R_{Ref})^{m-1} \right) \end{pmatrix}, \quad (7)$$

with  $\vec{z}'$  the conjugate of  $z'$ . Please note, that  $\vec{\mathbf{T}}_m^{(n)}$  and  $\vec{\mathbf{T}}_m^{(s)}$  differ in their last and thus these are not analytic functions in view of  $|z'|^2$  and  $\vec{z}'$ .

## APPLICATION

### Measuring a Curved Magnet

The local toroidal multipoles allow evaluating the effect of the magnet curvature on the measurement results. The details will be given elsewhere. Here only the method is described by words. Basically the basis functions are integrated over the coil probe length, taking the local offset between the coil probe axis and the torus radius into account [2, 4]. The expressions found are lengthy but most of the terms contribution to the field description can be ignored for magnets of a curvature of SIS100 or similar.

In cylindrical circular coordinates a translation of the reference frame by  $d_x, d_y$  produces a ‘‘feed down’’ effect; in matrix form it is given by

$$\mathcal{L}_{n,m}^{dr} = \begin{pmatrix} n-1 \\ m-1 \end{pmatrix} \left( \frac{d_x + i d_y}{R_{Ref}} \right)^{n-m}; \quad (8)$$

thus the translated multipoles  $C'_n$  are given by

$$C'_n = C_n \mathcal{L}_{n,m}^{dr}. \quad (9)$$

One finds however that the length of the coil probe gives the main effect and creates spurious harmonics, similar to the effect as found for cylindrical circular multipoles, given by

$$\mathcal{L}_{n,m}^{dr} = \underbrace{\frac{3R_{Ref} (d_x + i d_y)}{L_s^2 \epsilon (n-m)}}_{L_s} \mathcal{L}_{n,m}^{dr2}, \quad (10)$$

with the feed down, expressing the sum as matrix and  $\mathcal{L}_{n,m}^{dr2} = \frac{d}{dz} \mathcal{L}_{n,m}^{dr}$  with  $z = x + iy$  and  $d_x, d_y$  the offset of the coil rotating axis from the torus at the torus centre.

$L_s$  gives the relation between these bands

$$L_s = \sqrt{3 (d_x + i d_y) R_{Ref} / \epsilon} = \sqrt{3 (d_x + i d_y) R_C}, \quad (11)$$

using only the first side band ( $n-m == 1$ ). As one can see the to be chosen coil length  $L_s$  becomes smaller when the displacement errors  $d_x$  and  $d_y$  get smaller. On the other hand a smaller  $d_x$  or  $d_y$  will create smaller total spurious harmonics, and thus the overall contribution gets small. Therefore it is recommended to evaluate the above equation for the maximum tolerable deviations  $d_x, d_y$ . If a longer coil probe is chosen more effort shall be taken to determine  $d_x$  and  $d_y$ . Evaluating the above equations one finds that for SIS100 a coil length  $L = 2L'$  of  $\approx 600$  mm is acceptable.

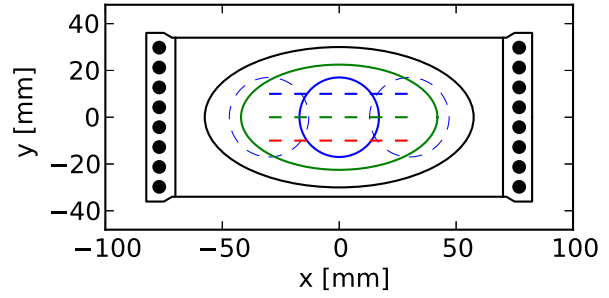


Figure 1: Location of the coil probes (blue circles) within the magnet aperture together with the ellipse (in green) used for calculating the elliptic multipoles. The larger black ellipse gives the intended good field region. The straight dashed lines show the area covered by the mapper and its hall probe. The other lines depict the magnet aperture together with the 8 turn coil (each turn shown as black circle).

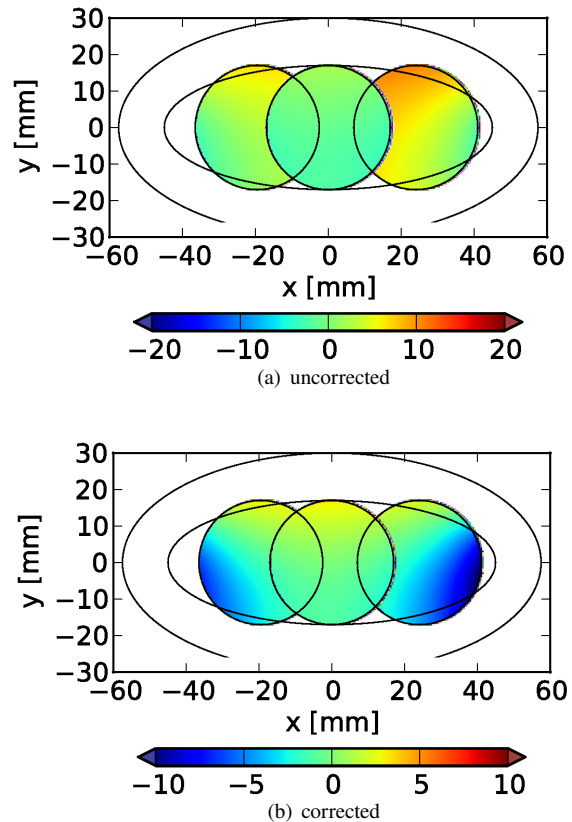


Figure 2: Corrected and uncorrected data as measured by the rotating coil probe for the field homogeneity  $B_y$ . Colour scale in units.

### Combining Rotating Coil Probes

If one interpolates the field using overlapping coil probe measurements (see Fig. 1), one will find that a significant difference in field is found between the two measurements (see Fig. 2) [1]. These difference are due to the fact that the

harmonics can only be determined with limited accuracy and in particular if a coil probe with compensation arrays (or “bucking windings”) are used. Thus in a first step the gain of the integrator  $g$  and the angle of the coil probe  $\beta$  is adjusted within their measurement accuracy, so that the

$$\mathbf{C}_m = \left(1 + \frac{g}{10\,000}\right) \bar{\mathbf{C}}_m e^{i(m+1)\beta}$$

fields match (see Fig. 2(b)). The multipoles are then computed combining the different measurements

$$\mathbf{B}_i(\mathbf{z}) = \lambda \sum_{m=1}^{M_m} \mathbf{C}_m^c \left(\frac{\mathbf{z}}{R_m}\right)^{m-1} + (1-\lambda) \sum_{m=1}^{M_m} \mathbf{C}_m^{l,r} \left(\frac{\mathbf{z} - x_m}{R_m}\right)^{m-1} \quad (12)$$

with a weighting function which is a cubic polynomial approximating the weight (or inverse error) of each measurement [1]. Using this polynomial the field can be reconstructed on the ellipse and elliptic multipoles can be calculated. These were used to reconstruct the field and compare it to the field measured by a hall probe mounted on an x-y-z mapper (see Fig. 3(a) for the end field and Fig. 3(b) for the central field). One can see that the field reconstructed by the combined coil probe measurement, and the one obtained by the mapper are in fairly good agreement for the end. In the central part a certain offset is to be seen but some deviation is found for the central part. The mapper could only cover a part of the length the coil probe covered, and thus the comparison is not for the same field. One can further see that there is some significant difference between to the ones predicted by calculations. The vertical field offset is a strong indication of a skew quadrupole, which can be also seen in the coil probe measurements; a field artefact, which would be passed, if the field would only be measured at the mid-plane of the magnet. Further the coil probe measurements show a clear indication of a significant skew sextupole.

## CONCLUSION

The rotating coil probe measurement method has been extended from its original use, for measuring straight magnets with a round aperture to curved magnets and an elliptic beam aperture. This method has been found working and allows understanding artefacts of the SIS100 dipole magnet [5], which could have otherwise slipped and only discovered during beam operation.

## ACKNOWLEDGMENT

The authors want to thank all how have contributed to this paper, either in direct form or by operating the test station systems, mounting the magnet on the bench or conducting the measurement, evaluating the data next to giving help or advice of any kind.

## REFERENCES

[1] P. Schnizer et al., NIMA, 607(3):505 – 516, 2009.

[2] P. Schnizer et al., COMPEL, 28(4), 2009.

[3] P. Schnizer et al., “Magnetic field description in curved accelerator magnets using local toroidal multipoles”, IPAC’11, San Sebastián, September 2011, WEPC060 (2011) <http://www.JACoW.org>

[4] P. Schnizer et al., “Toroidal circular and elliptic multipole expansions within the gap of curved accelerator magnets”, IGTE’10, Graz, September 2010.

[5] E. Fischer et al., “The SIS100 superconducting fast ramped dipole magnet”, IPAC’14, Dresden, Germany, June 2014, WEPRI083, These Proceedings.

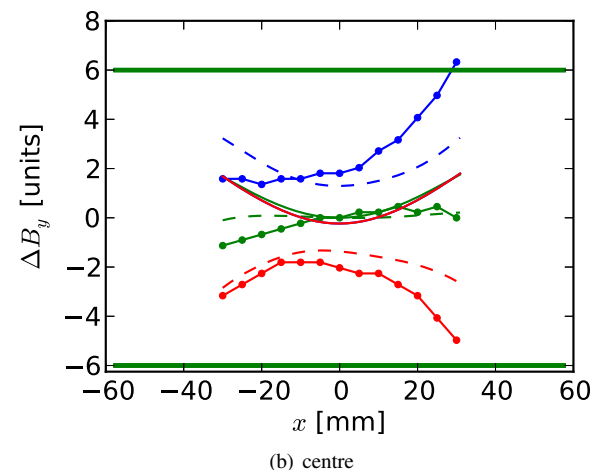
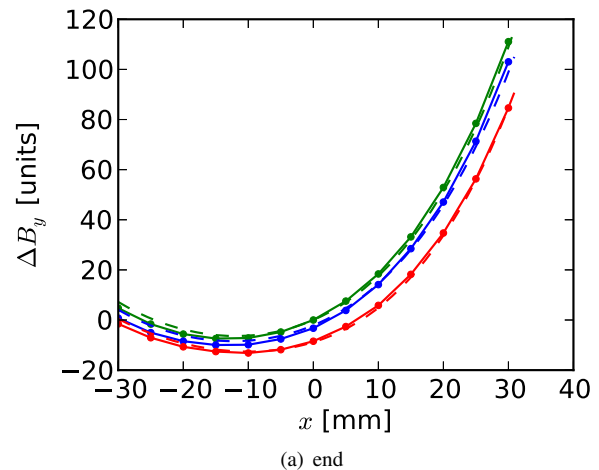


Figure 3: Comparison of the mapper data to the coil probe data. The dots indicate the mapper data (connected with lines, blue...  $y = +10$  mm, green...  $y = 0$ , red...  $y = -10$  mm), the dashed lines the reconstructed field for the magnet end (top) and centre (bottom). The field deviation of 600 ppm is indicated by the thick solid green lines in the lower plot, next to the calculated field in-homogeneity for a magnet without mechanical artefacts (solid lines).